Journal of Inorganic and Organometallic Polymers and Materials (2018) 28:2730–2741
https://doi.org/10.1007/s10904-018-0932-6

Investigation on Electrochemical Behavior and Catalytic Function of Glassy Carbon Electrode on the Basis of Magnetic Nano-particle with Simultaneous Incorporation of Myoglobin and Electron Mediator

Han Zeng[1] · Yu He Zhang[1] · Ting Mei Ma[1] · Wen Shan Huo[1]

Received: 2 June 2018 / Accepted: 23 July 2018 / Published online: 26 July 2018

Abstract
As-prepared magnetic nano-composite with Fe_3O_4 as core and carboxymethylated Chitosan as shell was proposed to act as matrix to co-immobilize electron relay and myoglobin by the means of chemical coupling. Subsequently Mb based bio-cathode was fabricated through the procedure of drop-casting in the presence of external magnet and was examined its performance in direct electron transferring and catalysis in electro-reduction of H_2O_2 with spectrometric and electro-chemical methods. Analysis in results indicated adjacent complexations between hetero-atoms in polymer and cofactors in enzyme/redox site of electron mediator would pose great impact on spectroscopic and electrochemical features of immobilized protein. These interactions would alter the path of electron shuttle and mechanism of catalysis.

Keywords Magnetic nano-composite · Electron mediator · Myoglobin · Adjacent complexation · Electro-catalytic reduction of H_2O_2

1 Introduction

Efficient electron transferring between electro-active sites in bio-molecules (e.g. cofactors in redox enzyme) and conductive matrix, desirable capability in substrate binding and transformation of entrapped bio-molecules are key factors which restrain the performance of electro-chemical instrument on the basis of bio-macromolecules incorporation into nano-device. Relevant attempts have been made for decades in order to verify the optimal means of catalysis involved in the application of bio-molecule based electro-chemical apparatus and to confirm the rate determining step of the catalytic cycle [1–6]. Heme protein is a huge family of redox protein including myoglobin and hemoglobin with Fe ion as redox site and porphyrin as ligands which can catalyze the reduction of di-oxygen and hydrogen peroxide. It should be noted that the change in configuration for heme-group of redox protein after integration into nano-material could be investigated by spectrometric and electrochemical methods and the essence of change in configuration of cofactor in enzyme molecule has not been elucidated clearly so far. Impacts of some important elements (e.g. pH value of buffer solution, temperature of operation and concomitant chemicals) on the characteristics of structure, chemical property and kinetics of catalysis have been probed recently. Thus some valuable conclusions are made [7–9]. For example: exposure extent of heme group determines the efficiency of inter-molecular electron transfer [9]. However influences of complicated interactions between enzyme carriers and incorporated protein molecules on physico-chemical features and configuration of immobilized protein molecules still remain to be explored further.

Magnetic nano-particle is an excellent candidate for integration of bio-macromolecules such as redox proteins, nucleic acid, lipids and saccharides to prepare bio-molecule based electro-chemical instrument because of good bio-compatibility, outstanding paramagnetism, low toxicity and desirable conductivity [10–13]. A series of nano-composites on the basis of magnetic Fe_3O_4 as core have been employed to tether electron mediator and/or enzyme molecule and then enzyme based nano-devices with favorable performance in energy out-put and chemical monitoring have been prepared successfully. Chitosan possesses the nature

✉ Han Zeng
zenghan1289@163.com

[1] Engineering Centre of Electrochemistry, Chemistry and Chemical Engineering Academy, XinJiang Normal University, 102# Xinyi Road, Urumuqi, Xinjiang 830054, People's Republic of China

of porosity which facilitates the mass/charge transferring and the enzyme accommodation. Furthermore, it should be supplemented that groups on the side chain of Chitosan such as –OH and $–NH_2$ would enhance the capacity of matrix to enzyme incorporation. Finally it should be noted that Chitosan and its derivatives have advantage of favorable biocompatibility and excellent function of film-formation which would promote the fabrication of enzyme-based electrode via drop-casting. Influence of interactions between constituents of nano-composite and redox protein/electron relay on kinetics and mechanism of enzyme-induced catalysis needs to be studied further because these complicated interreactions could pose impact on charge density of surface, strength of chemical bond and configuration of active site in enzyme molecule/electron relay. However investigation concerning about these issues has not been made adequately so far [14, 15]. Especially distinct spectroscopic features and electro-chemical behaviors for the incorporation of redox protein molecules into the similar matrix made up of magnetic nano-particle as core and different shell (polymer, nano-material and other inorganic chmicals such as SiO_2) with surface anchored electron relay (i.e. completely different absorbance band, conductivity, route of electron shuttle and rate of substrate attachment and conversion) have been identified for variable families of redox protein. Role in mechanism of catalysis for components of nano-composite should be probed indepth and relevant discussions have been less demonstrated until present [16, 17].

Magnetic nano-particle consisting of Fe_3O_4 as core and derivative of natural polymer: Chitosan as shell was proposed to be enzyme supporter for its advantages referred previously. Electron mediator and redox protein were co-immobilized into nano-particle through covalent linkage and then enzyme based electrode was fabricated to act as bio-cathode in potential glucose/di-oxygen bio-fuel cell and bio-electro-chemical monitor to detect the content of some oxidants such as hydrogen peroxide and di-oxygen. Dependence of features in electron transferring and catalytic function to reduction of H_2O_2 for entrapped heme protein on changes in structure parameters of nano-composite (i.e. such as forms of chemical bonds on the surface of protein, coordination geometry of co-factors within enzyme molecules and nature of interface of nano-composite) before and after protein accommodation was characterized by spectroscopic and electro-chemical means in this submission. Moreover subtle influences of so-called "adjacent co-ordination" on characteristics of electron transmission for immobilized enzyme molecules and conductivity of nano-composite were discussed in this manuscript and less investigation concerning about this issue has been performed up to now. It should be noticed some results from experiments were distinguished from those ones demonstrated previously. All these indicate the role of elements in nano-material could not be ignored.

2 Experiment

2.1 Reagents and Apparatus

Myoglobin from horse heart (Mb, Molecular mass 17,200) and carboxymethylated Chitosan (CMCH) are acquired from Macklin biochemical Co., Ltd. Shang-Hai of China and are used as available without extra purification. Ferrocene mono-carboxylic acid (FMCA, purity: 97%) is bought from Sigma-Aldrich chemical reagent Co., Ltd, USA and is put to application without any pretreatment. *N*-ethyl-*N*′-(3-dimethylaminopropyl) carbodiimide (EDC), glutaraldehyde (v/v = 1:1, aqueous system) and *N*-hydroxy succinimide (NHS) are secured from Shanghai Aladdin Reagent Co., Ltd, China. Other conventional reagents in this article are legal, available on market and are of analytical grade without additional declaration. Indium tin oxide (ITO) glassy panels are purchased from Nanjing Pioneer nano Material Technology Co., Ltd, China. Buffer solution throughout the experiments is 0.2 M phosphate buffer (PBS). pH value of PBS is modulated through the adjustment in concentration scale of KH_2PO_4 versus trisodium citrate. PBS is prepared with Milli-Q ultrapure water with resistivity higher than 18 MΩ cm. Commercial N_2 and O_2 with high purity are from Kangdi special gas Co., Ltd in China.

2.2 Preparation of Magnetic Nano-composite with Incorporated Mb as Well as Electron Relay and Protein-Based Biocathode

Magnetic Fe_3O_4 nano-particle was synthesized according to the description elsewhere [11]. Magnetic nano-particle over-lapped by CMCH was prepared as the procedure introduced previously [18] (denotation as CMCH@Fe_3O_4). It was stored under ambient temperature and local pressure for further application such as characterization and preparation of enzyme based electrode.

Basal electrode of glassy carbon electrode (diameter of 4 mm, GCE purchased from Aida Co, Ltd. in Tianjin, China) was pre-treated as previous demonstration [19]. 15 mL glutaraldehyde solution (volume of ratio in aqueous solution: 50%) was added into dispersed phase of CMCH@Fe_3O_4 to introduce aldehyde group which can tether redox protein molecules covalently through the formation of Schiff base. Subsequently PBS solution (pH 6.0, 75 mM EDC + 15 mM NHS) with content of Mb at 2.0 g L^{-1} and ethanol solution containing 0.1 M FMCA was added into the mixture successively to prepare magnetic nano-composite with simultaneous tethering of electron relay and redox protein molecule (designation in the

form of Mb/FMCA-CMCH@Fe_3O_4). Eventually drops of this nano-complex with integrated Mb was dripped onto the interface of basal electrode in the presence of magnet force (i.e. external magnet, specific procedure was demonstrated elsewhere [20]) to achieve uniform distribution of nano-composte with Mb onto the surface of electrode. Then electrode over-coated with a layer of viscous fluid was dried under room temperature and local pressure. Thus Mb based electrode was secured and denoted to be Mb/FMCA-CMCH@Fe_3O_4/GC. As prepared enzyme based electrode was stored in refrigerator at 4 °C when not in use.

2.3 Characterization of Nano-complex with Integrated Mb and Mb-Based Electrode

Changes in morphology and dimension of magnetic nano-composite before and after protein coupling were characterized by scanning electron microscopy (SEM) and transmission electron microscopy (TEM). Morphology characterization was conducted on JSM-6700F type field emission scanning electron microscope (accelerating voltage ranging from 0.5 to 30 kV, Japanese electrical Co, Ltd. JEO) and AMT XR401 transmission electron microscope (accelerating voltage at 100 kV, commercial from Advanced Microscopy Techniques Company, USA). Variations in chemical micro-environment (chemical bonds on the surface of enzyme molecules, configuration of redox site in protein molecules and/or valence state of cofactors within protein molecules before and after Mb incorporation into matrix) were investigated by UV–Vis as well as FT-IR. Change in electrical conductivity of magnetic nano-complex based electrode before and after Mb integration was probed by electrochemical impedance spectrometry (EIS) and AC impedance tests were conducted on Zahner Zennium electrochemical platform (Kronach, Germany, open circuit voltage at 0.459 V, range of frequency: 0.5–10^5 Hz, amplitude for excitation signal at 5 mV and 5.0 mM $K_3[Fe(CN)_6] + 0.1$ M KCl as electrochemical probe). Mechanical strength of Mb-based electrode was evaluated by graphite furnace atomic adsorption spectrometer (Analyst 800 type bought from Perkin–Elmer Company in USA, scanning range from 190 to 870 nm) according to the same procedure as previous demonstration [21]. Thermal stability of magnetic nano-composite was investigated by thermogravimetric analyzer (TGA, STA409 PC synchronous thermogravimeter was purchased from Netzsch Co., Ltd in Germany) and experiments were performed under such conditions as following: N_2 atmosphere, rate of temperature programming: 25 °C min^{-1} and temperature ranging from 298 to 1173 K.

2.4 Investigation in Electro-Chemical Behavior and Catalytic Effect on Reduction of H_2O_2 of Mb-Based Electrode

Electro-chemical behavior of electrode on the basis of FMCA functionalized magnetic nano-composite as well as catalytic efficiency on reduction of hydrogen peroxide for enzyme-based biocathode were investigated by cyclic voltammetry (CV) and chronoamperometry (CA) in combination with the technique of rotating disk electrode (AFMSRCE spinning disk electrode apparatus acquired from Pine Co. Ltd., USA. range of rotating rate: 50–10,000 rpm and temperature range of operation: 10–40 °C). Performance of mediated reduction of hydrogen peroxide for Mb-based electrode was characterized quantitatively with the difference in current of limiting diffusion under variable status (i.e. current recorded under deaerated PBS with or without substrate for steady *i–E* curves $|i_{substrate} - i_{blank}|$). All electrochemical experiments were performed in a conventional electro-chemical cell consisting of three electrodes: Mb-based electrode as working electrode, saturated calomel reference electrode (SCE) and self-made platinum coil serving as auxiliary one. Electrochemical cell was linked to commercial CHI-1140A electro-chemical working station (purchased from Chen-Hua Co., Ltd. Shang-hai in China). All potentials in this paper were relative to normal hydrogen electrode (NHE) without extra declaration and tests were conducted in ambient temperature (20 ± 0.6 °C) and aboriginal pressure. Efficient conductive area for variable electrodes was determined according to previous description [22] and current density (dimension: μA cm^{-2}) was derived from normalization of measured current to effective area of electrical-wired interface.

3 Results and Discussion

3.1 Characterization of Nano-complex with Tethered Mb

TEM and SEM images of Fe_3O_4 magnetic nano-particle (A), magnetic nano-composite of CMCH@Fe_3O_4 (B), magnetic nano-composite functionalized with FMCA: FMCA-CMCH@Fe_3O_4 (C) and magnetic nano-particle with incorporated Mb: Mb/FMCA-CMCH@Fe_3O_4 (D) were displayed in Figs. 1 and 2. As can be seen from Figs. 1 and 2 of this paper, spherical shape of as-prepared magnetic nano-particle of Fe_3O_4 was recognized with average diameter within the range of 5–10 nm (see Figs. 1a, 2a. Dimension of magnetic particle was smaller than that with the similar shape shown previously [11]). Accumulated clusters with amorphous outline and large dimension could be detected for magnetic nano-composite of CMCH@Fe_3O_4 (see Figs. 1b, 2b) which

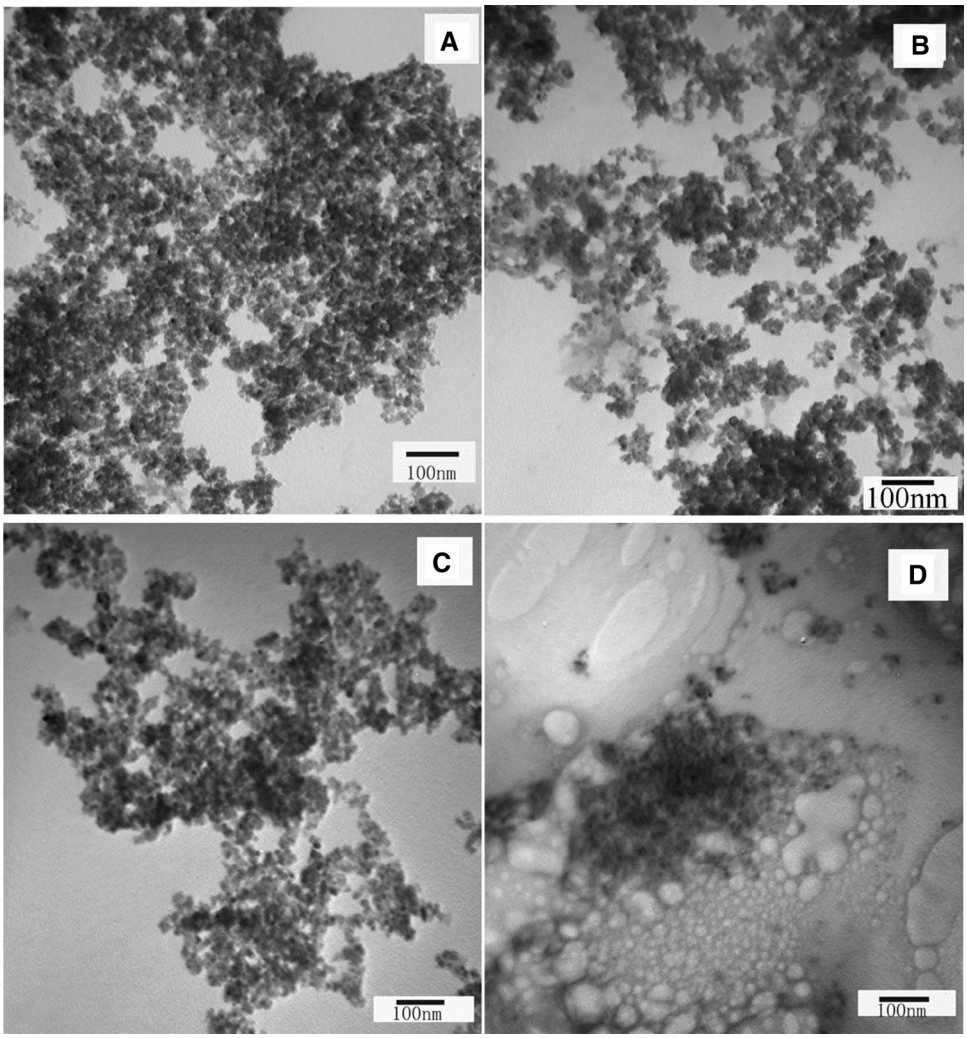

Fig. 1 TEM images of magnetic nano-particle: Fe_3O_4 (**a**), nano-composite: CMCH@Fe_3O_4 (**b**), electron relay surface-functionalized magnetic nano-composite: FMCA-CMCH@Fe_3O_4 (**c**) and magnetic nano-particle with anchored FMCA and immobilized Mb: Mb/FMCA-CMCH@Fe_3O_4 (**d**)

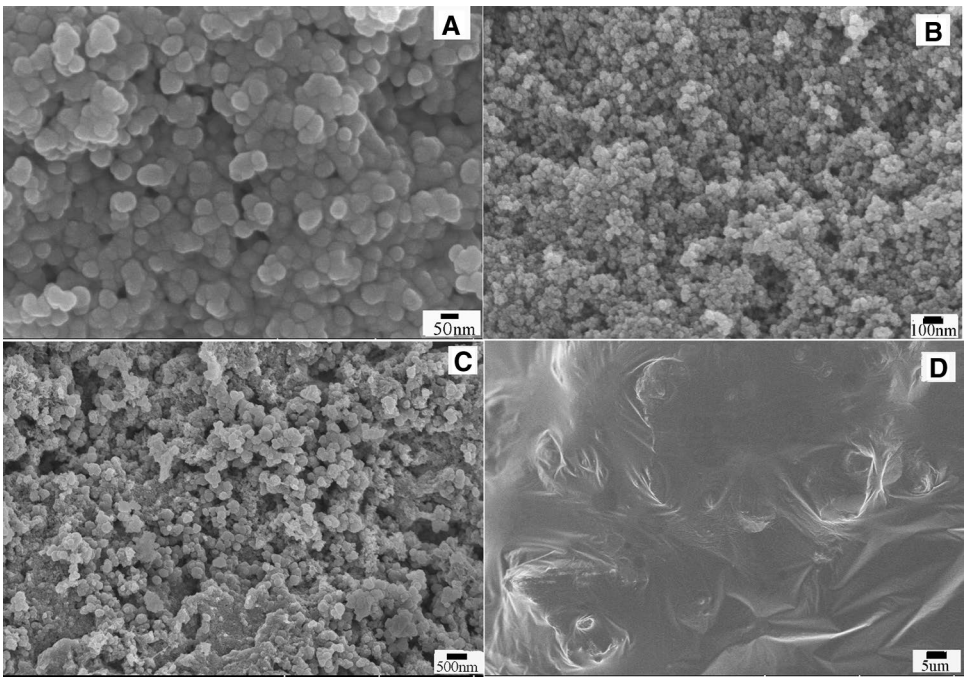

Fig. 2 SEM images of Fe_3O_4 (**a**), CMCH@Fe_3O_4 (**b**), mediator modified nano-composite: FMCA-CMCH@Fe_3O_4 (**c**) and magnetic nano-particle surface-tailored with FMCA and Mb: Mb/FMCA-CMCH@Fe_3O_4 (**d**)

resulted from the hydrogen bond formation between some groups such as carboxyl groups, amino groups and hydroxyl groups. This result was in accordance with that demonstrated previously [18]. Relatively regular morphology with quasi-spherical shape for part of FMCA-CMCH@Fe_3O_4 (see Figs. 1c, 2c) can be observed because of orientated array for surface tailored magnetic nano-composite originating from π–π stacking effect of hydrophobic aromatic ring linked to the polymer unit. Morphology of magnetic nano-particle with integrated Mb (Mb/FMCA-CMCH@Fe_3O_4, see Figs. 1d, 2d) was more sophisticated in that some quasi-spherical nano-particles with bigger size were distinguished from other abnormal clots. Former structure should be ascribed to complicated interactions between enzyme/electron relay and matrix. These interactions are comprised of hydrogen bond, π–π stacking effect of hydrophobic sites and complexations between active site in Mb (i.e. metal ion within Mb molecule)/Fe ion within mediator functionalized on the surface of magnetic nano-particle and hetero atoms in block unit of polymer. It suggested these interactions would not only influence the morphology of nano-composite with entrapped redox protein molecules but also would pose impact on spectroscopic and electrochemical characteristics of nano-complex with Mb integration.

FTIR spectra of free Mb, nano-composite modified by electron relay: FMCA-CMCH@Fe_3O_4 and magnetic nano-particle surface-anchored with FMCA as well as Mb: Mb/FMCA-CMCH@Fe_3O_4 were shown in Fig. 3A. It was apparent from Fig. 3A absorption peaks at 1606.6, 1419.3 and 515.0 cm^{-1} of stretching vibrations of C=O, C–O–C for the formation of ester and Fe–Cp ring for ferrocenyl unit were identified for FMCA-CMCH@Fe_3O_4. Blue shift of ~20 nm relative to the absorption band of Fe–Cp ring in FMCA (data not shown) for the same functional group in FMCA-CMCH@Fe_3O_4 should be attributed to the linkage of Fe–Cp ring with carbonyl group in ester. While red shift in stretching vibration peak of carbonyl group and blue shift in stretching vibration peak of C–O–C in ester for FMCA-CMCH@Fe_3O_4 relative to CMCH@Fe_3O_4 (FTIR of CMCH@Fe_3O_4 was displayed previously [18] and analysis in FTIR of CMCH@Fe_3O_4 indicated covalent linkage between Fe_3O_4 and Chitosan could be achieved through the formation of amido bond and the absence of coordination between magnetic nano-particle and hetero-atoms in Chitosan) may originate from the conjugation effect in existence of adjacent Fe–Cp ring and abutting complexation of metal ions in ferrocenyl groups with hetero-atoms in polymer respectively. FTIR of Mb/FMCA-CMCH@Fe_3O_4 was more complicated in that less blue shift in stretching vibration peak of Fe–Cp ring (~522.0 cm^{-1}) and apparent red shift in characteristic peak of C=N in Schiff base at 1628.1 cm^{-1} relative to that described elsewhere [10] (1656.0 cm^{-1}) were confirmed. The former could be attributed to the consequence of adjoining ligation depicted previously in

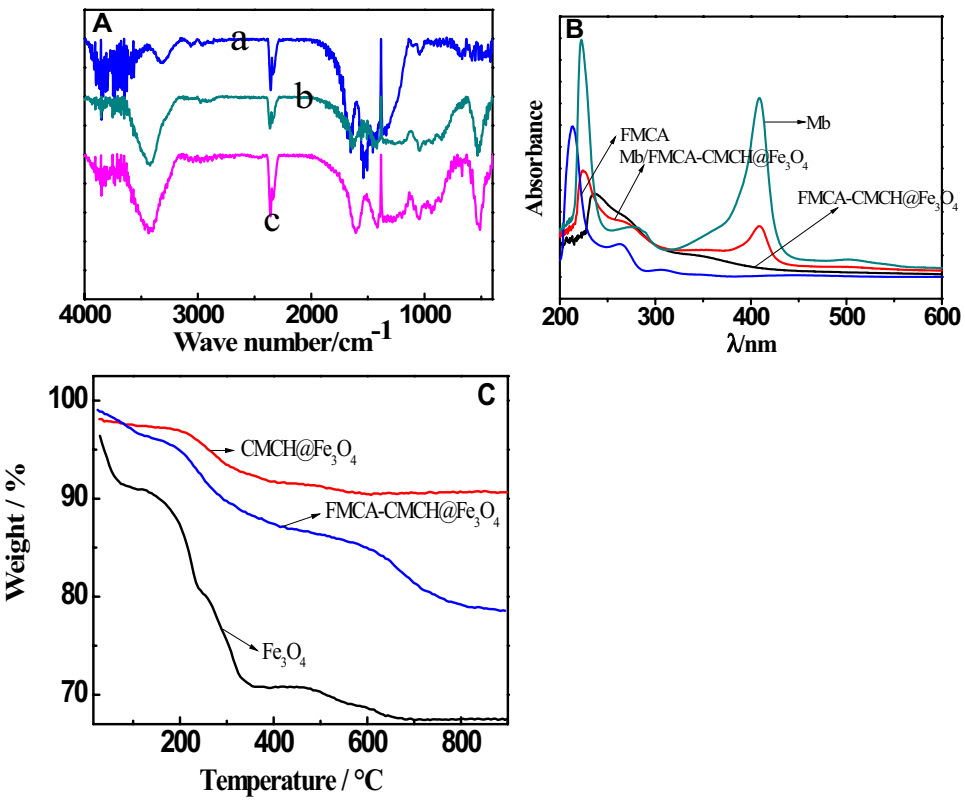

Fig. 3 **A** FTIR spectra of free Mb (*a*), magnetic nano-particle with immobilized FMCA and Mb: Mb/FMCA-CMCH@Fe_3O_4 (*b*) and magnetic nano-composite modified by electron mediator: FMCA-CMCH@Fe_3O_4 (*c*); **B** UV–Vis spectra of free Mb, solution containing electron relay: FMCA, thin film of FMCA-CMCH@Fe_3O_4 and thin membrane of nano-composite with tethered Mb and FMCA: Mb/FMCA-CMCH@Fe_3O_4; **C** thermogravimetric curves (TG) of magnetic nano-particle: Fe_3O_4, nano-composite: CMCH@Fe_3O_4 and nano-composite surface-modified by electron relay: FMCA-CMCH@Fe_3O_4

the presence of conjugation system (porphyrin ring in Mb molecule) and latter could be ascribed to conjugation effect which averages the density of electron. It should be noted that other peaks of Mb/FMCA-CMCH@Fe_3O_4 were similar to that of free Mb and magnetic fluid. It can be deduced from analysis that electron relay and redox protein were successfully immobilized on the surface of magnetic nano-particle and other surface groups of enzyme molecules were intact. Furthermore adjacent complexation of Fe ion in ferrocenyl group or Mb with hetero-atoms in polymer may pose considerable impact on the configuration of active site in protein or anchored electron mediator, the dynamics of electron shuttle between redox active species and conductive support together with the catalytic mechanism of enzymatic reaction.

Usually UV–Vis spectroscometry was considered to be an efficient way to explore the influence of interactions between enzyme carrier and immobilized protein on physical and chemical properties of enzyme molecules. UV–Vis spectra of free Mb, ethanol solution with FMCA, nano-composite surface modified by electron relay and magnetic nano-particle with co-immobilized FMCA and Mb were shown in Fig. 3B. It can be seen from Fig. 3B that three distinct absorption bands could be recognized (two of them located at 222.6 and 409.6 nm were strong and sharp and the third one emerged at ~ 284.0 nm was broad and faint) for free Mb. They should be ascribed to π–π* electron transition for porphyrin ring in Mb, d–d coordination transition of electrons within d orbital for Fe ions of Mb in the presence of hetero-atoms (for example: N or O atoms, this result was in accordance with that demonstrated early [23]) and n–π* electron transition for peptide linkage of protein molecules, respectively. Three distinguished absorption peaks with subsequently diminished area were discerned in UV–Vis spectrum of ethanol solution containing FMCA. Two bands of them located at 214.1 and 264.3 nm could be classified into the typical π–π* electron transition of Cp ring in FMCA molecule and the third one at 303.7 nm should be attributed to d–d coordination transition of d electron transfer for Fe ion within electron mediator in the presence of Cp ring. Absorption bands for π–π* electron transition of Cp ring in FMCA molecule disappeared completely and the new absorption peak with weak signal emerged at 236.5 nm could be ascribed to adjacent complexation described previously which occurred between Fe ion in FMCA and neighboring hetero-atoms (i.e. O atoms in ester linkage formed on the surface of nano-composite) for nano-composite with surface-functionalized FMCA. It meant the original conjugation of Fe–Cp ring of FMCA would be distorted after covalent linkage of FMCA to nano-composite of CMCH@Fe_3O_4. It also suggested the capability of electron transfer for FMCA immobilized on CMCH@Fe_3O_4 would be crippled to some extent. Finally the spectra of magnetic nano-particle with surface-tailored FMCA and Mb was more sophisticated than those ones discussed previously in that similar absorption bands at 408.8 and 224.9 nm for d–d complexation transition of Fe ion in Mb and n–π* electron transition within peptide described previously could be detected. While signals which were representative of π–π* electron transition for Cp ring in FMCA and adjoining ligation between metal ion in FMCA and its peripheral hetero-atom demonstrated earlier could not be discerned. It can be deduced reasonably from analysis in Fig. 3B that the basic structure of enzyme molecule was intact in spite of the formation of Schiff base and the interaction between enzyme and protein carrier may interfere with the abutting coordination referred previously, indicating unique electro-chemical characteristics of redox groups anchored on the surface of magnetic nano-particle with Mb immobilization.

TG curves of magnetic nano-particle: Fe_3O_4, core–shell nano-composite: CMCH@Fe_3O_4 and nano-composite with surface-anchored electron mediator: FMCA-CMCH@Fe_3O_4 were exhibited in Fig. 3C. Analysis in Fig. 3C revealed that the procedure of thermal decomposition for magnetic nano-particle: Fe_3O_4 could be classified into several steps: the first and the second one for evaporation of water molecule in the mode of adsorption or binding together with latter steps for break-down of ferroferric oxide (This conclusion could be confirmed by the ratio of weight-loss: ~ 67.5% of initial mass remained at termination temperature of thermal decomposition: 680 °C, indicating remnant at this temperature was only ferrum). Thermal decomposition initialed at ~ 230 °C for nano-composite: CMCH@Fe_3O_4 which was corresponding to the thermal resolution of side chain and depolymerization of backbone in polymer. While the case for FMCA-CMCH@Fe_3O_4 was distinguished from both demonstrated previously in some signals with slow rate and high temperature of decomposition identified in Fig. 3C for evaporation of H_2O molecule attachment on the interface of nano-composite in aid of hydrogen bond (this result was similar to that shown elsewhere [24]) as well as for degradation of surface tethered ferrocenyl structure unit. It can be easily deduced from analysis that the thermal stability of FMCA-CMCH@Fe_3O_4 was higher than bare Fe_3O_4 and nano-composite: CMCH@Fe_3O_4. This deduction was supported by the comparison in ending point for thermal decomposition of them: 750 °C for FMCA-CMCH@Fe_3O_4 and 575 °C for CMCH@Fe_3O_4. Better thermal stability of the former should be attributed to the presence of adjacent coordination between ferrocenyl group and neighboring hetero-atoms in polymer depicted early.

Mechanical stability of magnetic nano-particle with integrated Mb was evaluated through measurements in content of Fe under distinct cases (i.e. blank electrolyte in the absence of Mb, supernates from magnetic separation from mixtures of blank solution incubated adequately with nano-particle surface-anchored by Mb and FMCA or FMCA functionalized nano-composite under stirring at the

rate of 600 rpm for 6 min). Results from determinations showed that no apparent change in content of Fe could be detected and concentration of Fe in solution could not reach the detection limit of the monitor. Thus conclusion could be made that chemical coupling would greatly improve the mechanical stability of immobilized protein molecules and anchored redox groups for both systems.

3.2 Electrochemical Behavior and Performance in Catalysis of H_2O_2 Reduction for Mb Based Electrode with Magnetic Nano-particle as Support

EIS spectra of naked GCE, CMCH@Fe_3O_4/GC, FMCA-CMCH@Fe_3O_4/GC, electrode over-coated by nano-composite with Mb incorporation alone: Mb/CMCH@Fe_3O_4/GC and Mb/FMCA-CMCH@Fe_3O_4/GC in electrolyte containing electro-chemical probe, were demonstrated in Fig. 4a. Accordingly CV plots of those electrodes in the same system recorded at the potential sweeping rate of 100 mV s^{-1} were shown in Fig. 4b. Conclusion could be drawn from Fig. 4a that the efficiency of electron shuttle would be enhanced in the presence of magnetic nano-particle and surface anchored electron mediator and capability of electron transferring would be hindered greatly after Mb incorporation into magnetic nano-particle or nano-composite resulting from the existence of huge and insulated backbone of protein. This conclusion was on the basis of fact those electrodes were arrayed in the order of elevation in charge-transferring resistance as following: FMCA-CMCH@Fe_3O_4/GC, CMCH@Fe_3O_4/GC, bare GCE, Mb/CMCH@Fe_3O_4/GC and Mb/FMCA-CMCH@Fe_3O_4/GC. Result in analysis of CVs for those electrodes (order of elevation in current responses for electro-active species on those electrodes) from Fig. 4b was in accordance with that derived from analysis in EIS spectra substantially except for FMCA-CMCH@Fe_3O_4/GC. The exception could be blamed for abutting complexation referred early which resulted in the depression in process of reversible charge-transferring for electro-active probe (i.e. blockage

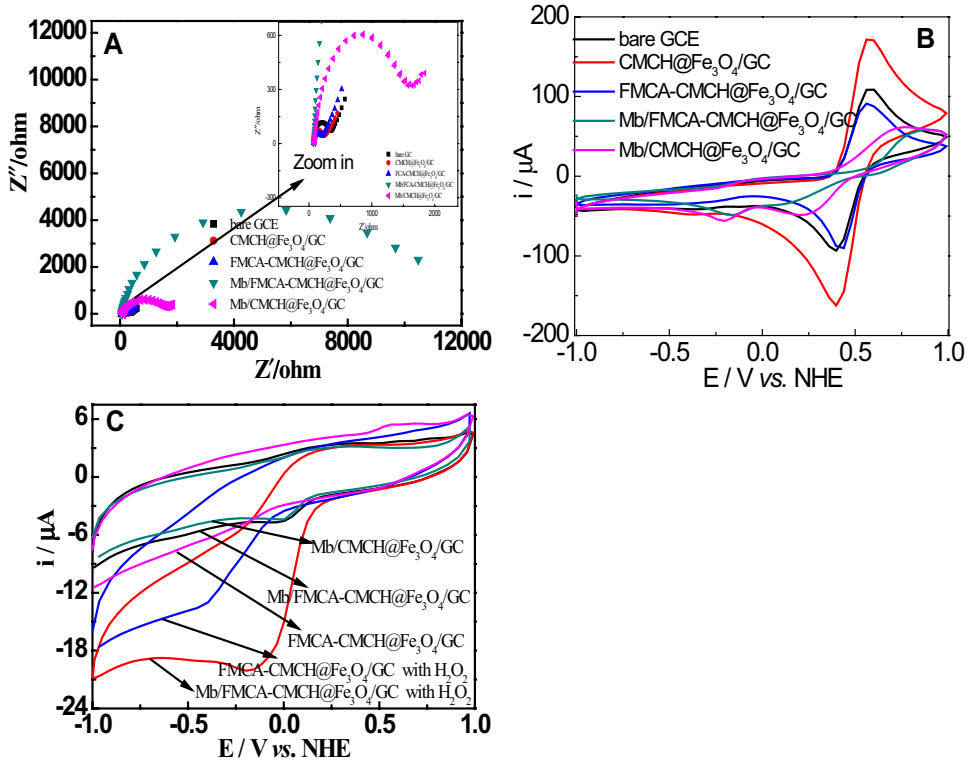

Fig. 4 **a** EIS spectra of naked supporting electrode, nano-composite modified electrode, electrode on the basis of nano-composite with tethered electron mediator, electrode based on the magnetic nano-particle with electron relay and Mb co-immobilization and electrode capped by nano-composite with Mb integration in electrolyte containing electro-chemical probe (i.e. 5 mM $K_3[Fe(CN)_6]$ + 0.1 M KCl), **b** cyclic voltammograms (CVs) of bare GCE, CMCH@Fe_3O_4/GC, FMCA-CMCH@Fe_3O_4/GC, Mb/FMCA-CMCH@Fe_3O_4/GC and Mb/CMCH@Fe_3O_4/GC in solution with electro-active species; **c** CVs of basal electrode modified by nano-composite with Mb incorporation, electrode over-coated by thin film of FMCA functionalized nano-composite and electrode capped by magnetic nano-particle with FMCA and Mb integration in N_2 purged PBS (pH 7.0) without or with hydrogen peroxide (content of H_2O_2 was 0.420 mM) recorded in static status and at the rate of 50 mV s^{-1}

of electron approach from electro-active species to conductive support) to a certain extent.

CVs of Mb/CMCH@Fe_3O_4/GC, FMCA-CMCH@Fe_3O_4/GC and Mb/FMCA-CMCH@Fe_3O_4/GC in deaerated PBS (pH 7.0) recorded under different cases: in the presence and in the absence of hydrogen peroxide were shown in Fig. 4c. Results from analysis in Fig. 4c indicated that a pair of redox wave with blunt shape of oxidation peak and sharp reduction one was verified for both electrodes: Mb/CMCH@Fe_3O_4/GCE and Mb/FMCA-CMCH@Fe_3O_4/GCE which was distinct from that of CMCH@Fe_3O_4/GCE described elsewhere [18]. Considering the absence of any distinguished signal of redox process for CMCH@Fe_3O_4/GCE, redox peaks referred earlier could be regarded to be the direct electron shuttle between active site in Mb: heme and conductive matrix with inferior reversibility and dynamics of redox process. Figure 4c also provided the side proof to support the assumption that the existence of adjoining ligation between Fe ion in ferrocenyl group and peripheral hetero-atoms in polymer would cripple the electron shuttle between redox species dissolved in electrolyte and electrode partly. It can be seen from Fig. 4c prominent reduction wave emerged at ~ − 40 mV and a series of oxidation waves with distinct outline for Mb/FMCA-CMCH@Fe_3O_4/GCE could be identified. Furthermore similar oxidation waves and single reduction wave with blunt peak at ~ 505 mV (i.e. the signal of reduction process of oxidized FMCA) could be discerned for FMCA-CMCH@Fe_3O_4/GCE. It should be noted the mean peak of oxidation at 710–760 mV and diminished redox peaks at ~ 510 mV (the mid-wave potential of ferrocenyl group [25]) for CVs of two electrodes described previously could be considered to be proof indicating the existence of abutting ligation demonstrated early. This complexation would influence the redox process of active site in Mb or electron relay. Redox waves of Mb/CMCH@Fe_3O_4/GCE and Mb/FMCA-CMCH@Fe_3O_4/GCE were different completely from those described elsewhere [26, 27] with the same redox enzyme incorporation into variable matrices (only a pair of redox peak at ~ − 40 mV for active site in Mb could be discovered). It should be attributed to the interaction referred foregoing. Moreover both electrode of FMCA-CMCH@Fe_3O_4/GCE and Mb/FMCA-CMCH@Fe_3O_4/GCE displayed obvious catalytic function on reduction of H_2O_2 with variable onset potential of catalysis at ~ 445 and 520 mV (the case of Mb/CMCH@Fe_3O_4/GCE was similar to that of Mb/FMCA-CMCH@Fe_3O_4/GCE, data not shown). It indicated that the catalytic efficiency in reduction of H_2O_2 would be enhanced greatly after Mb incorporation into magnetic nano-particle with higher onset potential of reduction and elevated current of reduction peak. All these results suggested that the capability in electron transferring of FMCA would be crippled to a considerable extent and the affinity to substrate of immobilized Mb would be improved greatly in the presence of neighboring coordination.

Figure 5A, B demonstrated steady *i*–*E* curves of Mb based electrodes: Mb/CMCH@Fe_3O_4/GCE and Mb/FMCA-CMCH@Fe_3O_4/GCE in oxygen-free PBS (pH 7.0) without H_2O_2 recorded at different rate of potential scanning. Their inset graphs were corresponding correlation plots of anodic peak currents and cathodic peak ones versus square root of scanning rates. A pair of symmetrical redox wave with formal potential at ~ − 110 mV and single oxidation peak within the range from 365 to 425 mV at higher scanning rates (peak potential made a positive shift with the elevation in rate of potential sweeping and this signal could be considered to be the oxidation of Fe ion in reduced state for immobilized Mb in coordination with N atom in polymer on the surface of nano-particle) could be detected for Mb/CMCH@Fe_3O_4/GCE from Fig. 5A. While the case of Mb/FMCA-CMCH@Fe_3O_4/GCE in Fig. 5B was more sophisticated: a pair of redox peak with favorable reversibility and formal potential was identified at − 85 mV, two blunt oxidation wave (former was observed within the range from 400 to 450 mV, the relationship between potential and scanning rate was similar to Mb/CMCH@Fe_3O_4/GCE while the latter emerged at relatively stable potential: ~ 740 mV under variable scanning rates) and a single weak reduction one were localized at constant potential of ~ 680 mV under modulated sweeping rates. It can be deduced from Fig. 5A, B that direct electron transferring between heme of Mb and conductive support could be achieved with different formal potential which could be attributed to complicated interactions between cofactor in redox enzyme or tethered electron mediator and peripheral hetero-atoms of polymer on the interface of nano-particle. Distinguished quasi-reversible redox signal at formal potential of ~ 710 mV should be classified into a typical electrochemical process of Fe ion in ferrocenyl group in ligation with neighboring hetero-atoms. It should be noted that anodic and cathodic currents at formal potentials of active site in Mb: heme for both electrodes increased proportionally with the augment in square root of sweeping rates and difference of redox peaks also expanded slightly with the elevation in scanning rates. This revealed the fact that redox process of co-factor in Mb for both electrodes should be consistent with the typical behavior of thin film controlled prototype. Furthermore CVs of Mb/FMCA-CMCH@Fe_3O_4/GCE in oxygen-free PBS with variable consistency level of H_2O_2 were displayed in Fig. 5C. It could be drawn from analysis in Fig. 5C that the bell shape reflecting the dependence of peak current for catalytic reduction of H_2O_2 on content of substrate was observed. It indicated that Fe ion of Mb in the status of complexation with adjoining hetero-atoms

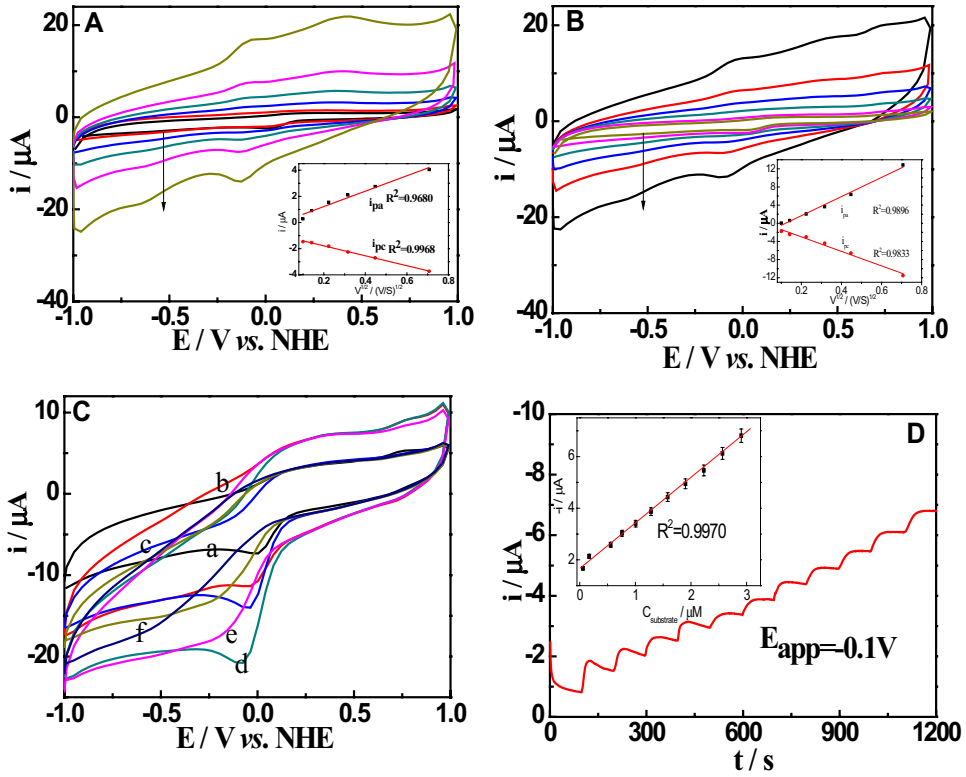

Fig. 5 CVs of electrode over-coated by nano-composite with Mb incorporation (**A**) and electrode modified by magnetic nano-particle with FMCA and Mb co-immobilization (**B**) in N_2-bubbled PBS (pH 7.0) recorded at variable scanning rates of potential and in the absence of substrate: H_2O_2, from inner curve to outer one indicating the sweeping rate: 2, 5, 10, 20, 50, 100 mV s^{-1}. Inset graph of **A**, **B** linear fitting curves of anodic peak currents and cathodic ones versus square root of sweeping rates for both Mb based electrodes; **C** CVs of Mb/FMCA-CMCH@Fe_3O_4/GC in deaerated PBS (pH 7.0) with alterable consistency level of hydrogen peroxide recorded at the sweeping rate of 50 mV s^{-1}, concentration of hydrogen peroxide for curve *a–f* 0.1399, 0.2797, 0.3636, 0.4196, 0.5874, 0.7832 mM; **D** chronoamperometric curve of Mb/FMCA-CMCH@Fe_3O_4/GC in N_2 saturated PBS containing variable concentration level of H_2O_2 determined at the applied potential of −0.1 V and in the mode of stirring electrolyte, its inset graph is the dependence plot of steady response in the form of catalytic current on content of substrate: H_2O_2

may bind O_2 originating from the dissociation of H_2O_2 (i.e. amount of oxygen molecule can not be ignored). Thus this combination of O_2 with active site in Mb: heme could hinder the approach of H_2O_2 to binding site of Mb (O_2 in binding state could not be reduced to H_2O at this positive potential [28]). This judgment may be justified as the same relationship between catalytic current and content of substrate could be identified for Mb/CMCH@Fe_3O_4/GCE and the case for FMCA-CMCH@Fe_3O_4/GCE was distinct from this: catalytic current rose with the ascension of substrate and then attained the maximum at higher content of H_2O_2 (data not shown). It should be underlined that the fact that the apparent change in consistency level of di-oxygen molecule in electrolyte can not be monitored. It could be regarded as side proof to support the conclusion illustrated previously. Figure 5D was the curve of steady current versus time lapse for Mb/FMCA-CMCH@Fe_3O_4/GC in stirring and deaerated PBS with alterable consistency of H_2O_2 under the constant potential. Inset graph of Fig. 5D was the calibration plot of steady current for catalytic reduction of H_2O_2 versus concentration of substrate. It can be deduced from Fig. 5D and its inset graph that the Mb based electrode was sensitive to the substrate with high sensitivity of 1.67×10^3 μA L $mmol^{-1}$ but slow response in comparison to other similar systems [23, 28]. It suggested the turn-over frequency of binding substrate was not favorable which was in accordance with the conclusion illustrated previously. However the affinity to H_2O_2 for Mb based electrode was excellent with low K_M (12.12 μmol L^{-1}, lower than those demonstrated elsewhere [29–31]. For instance: K_M of Nafion/Mb-SA-Fe_3O_4-GR/CILE to H_2O_2: 90.8 mmol L^{-1} [29]) which was derived from double reciprocal plot of steady current of catalysis versus content of substrate. Desirable capability of substrate binding for Mb based electrode should be attributed to the presence of the neighboring coordination described previously. It should be stressed that the good linear relationship could be retained within the range of substrate

Table 1 Dependence of catalytic efficiency in reduction of H_2O_2 (consistency at 0.3916 mM) for Mb/FMCA-CMCH@Fe_3O_4/GC on concentration ratio of myoglobin versus FMCA

Electrode	Consistency ratio of enzyme versus electron relay		Relative activity of catalysis (%)[a, b]
	Concentration of myoglobin (g L^{-1})	Concentration of FMCA (M)	
1[#]	0.5	0.1	31.8 ± 1.1
2[#]	1.0	0.1	64.9 ± 2.3
3[#]	2.0	0.1	100 ± 3.4
4[#]	3.0	0.1	76.9 ± 2.8
5[#]	5.0	0.1	43.1 ± 1.3
6[#]	2.0	0.02	47.9 ± 1.5
7[#]	2.0	0.05	81.7 ± 3.0
8[#]	2.0	0.1	100 ± 3.4
9[#]	2.0	0.2	73.6 ± 2.6
10[#]	2.0	0.4	34.5 ± 0.9

[#]Indicated the number of electrode which was prepared through the same procedure of preparation but with the distinct constitution

[a]It should be noted that relative activity was defined with the form of limiting catalytic current under certain concentration ratio of enzyme versus electron relay/maximum in limiting catalytic current under optimal consistency ratio of Mb versus FMCA

[b]An average of three replicate determinations

consistency (0.06–2.90 μmol L^{-1}) and the detection limit to substrate for this Mb based electrode was figured out to be 0.024 μmol L^{-1} which was lower than that demonstrated previously (1.0 μmol L^{-1}) [26].

Discussion for optimization in composition of materials employed for electrode modification was illustrated in Table 1. Results from Table 1 indicated only moderate concentration ratio of enzyme versus electron mediator (2.0 g L^{-1}: 0.1 M) could obtain most desirable catalytic efficiency after systematic evaluation (when the size of nano-particle was appropriate enough to allow adequate specific surface area and avoid the agglomeration of tethered bio-molecules as demonstration elsewhere [19]). Overfull enzyme could lead to agglomeration of immobilized Mb which would decrease the opportunity of substrate to approach active site of Mb and would depress the catalytic effect of enzyme to substrate. Similarly excessive electron mediator could cause the abatement in catalytic efficiency which originated from partial combination of FMCA with enzyme dissolved in electrolyte (i.e. it meant the reduction of incorporated bio-catalyst molecules in enzyme carrier and would cripple the function in electron shuttle of FMCA).

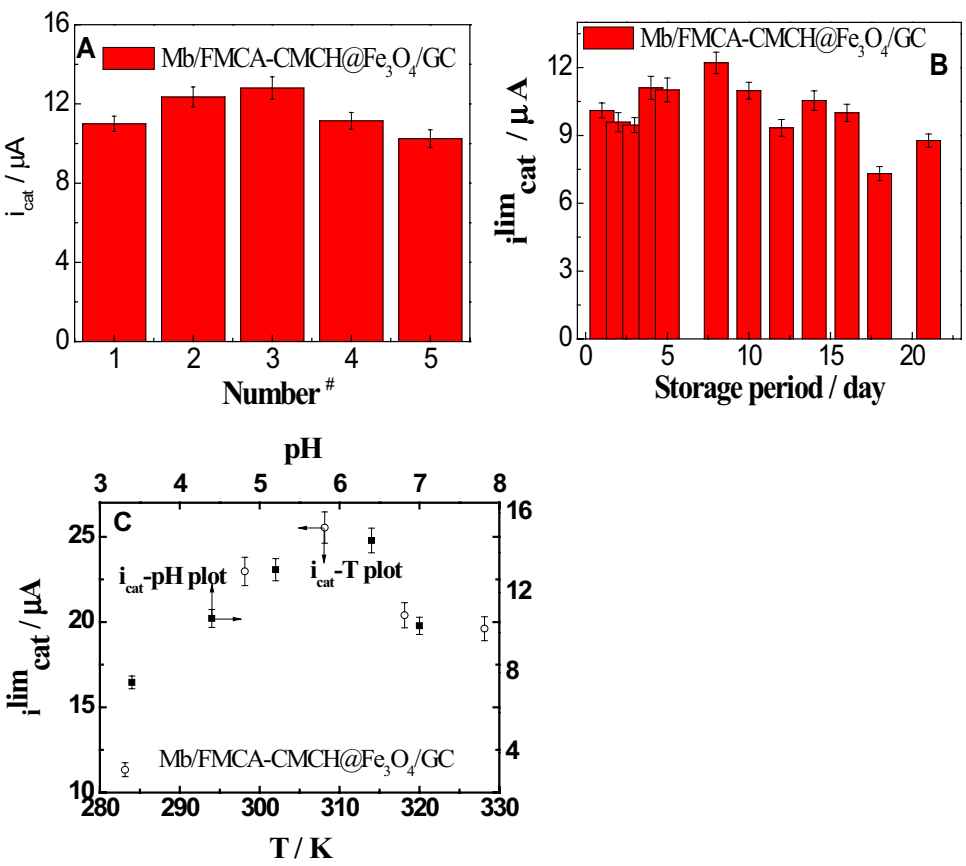

Fig. 6 Reproducibility (**a**), long-term usability (**b**), thermal stability and acid–base endurability (**c**) in catalysis of hydrogen peroxide for Mb/FMCA-CMCH@Fe_3O_4/GC, operating parameters in electro-chemical experiments were identical to those described in Fig. 5C except for the concentration of H_2O_2 at 0.3916 mM

3.3 Reproducibility, Long-Term Usability, Acid–Base Endurability and Thermal Stability in Catalysis of Hydrogen Peroxide for Mb Based Electrode

Limiting catalytic currents of five Mb-based electrodes (Mb/FMCA-CMCH@Fe_3O_4/GC) in nitrogen bubbling electrolyte with the same consistency level of substrate recorded at the constant potential and the identical sweeping rate of potential were exhibited in Fig. 6a. Results in Fig. 6a revealed that the difference among catalytic effects in reduction of H_2O_2 for Mb-based electrodes was trivial with RSD of 8.2%. Hence it showed that the reproducibility of this Mb-based electrode was favorable. Shrinkage in limiting current of catalytic reduction with time lapse for Mb-based electrode was displayed in Fig. 6b. It can be seen from Fig. 6b that the long-term usability was desirable generally with the characteristics of slow attenuation in catalytic activity. It should be noted that the residual activity of catalysis could be retained ~ 72.3% of initial value and the onset potential of electro-reduction didn't shift apparently even after storage over 2 weeks (the latter was confirmed after comparison in CVs of electrode at different time intervals, data not shown). Figure 6c depicted the relationships of limiting catalytic current versus pH value of buffer solution and operation temperature. Analysis in results from Fig. 6c indicated that the bell shape for dependence of catalytic function on pH and temperature of application was discovered for Mb based electrode. Results also illuminated that the optimal pH and temperature of application for Mb/FMCA-CMCH@Fe_3O_4/GC were distinguished from those ones for free Mb (the former and the latter were 6.4, 35 and 7.5, 40 °C [8] respectively). It should be ascribed to the unique characteristics of surface group and thermal sensitivity for magnetic nano-particle capped by polymer (i.e. partly ionized H^+ from groups on the side chain of polymer may enhance the electro-reduction of hydrogen reduction resulting from maintenance of the catalytic effect in the status of slight acidity). Analysis in result of electron shuttle test for electron mediator (FMCA) tethered to magnetic nano-particle also provided the convincing proof to back up the previous conclusion (i.e. maximum of apparent diffusion coefficient for electron relay was observed at 35 °C and it was in accordance with the low critical solution temperature of CMCH basically, data not shown).

4 Conclusion

Myoglobin and electron relay-ferrocene mono-carboxylic acid were co-immobilized on the interface of magnetic nano-particle: Fe_3O_4 functionalized by carboxymethylated Chitosan in the way of chemical coupling. Sophisticated interactions including adjacent coordination between active sites in enzyme or electron mediator and constituents of enzyme carrier would enhance the mechanical strength of nano-composite with protein and electron relay integration. These interactions would also pose considerable impact on spectroscopic and electro-chemical features as following: partially ordered structure for agglomeration of nano-particle with enzyme and electron mediator co-immobilization, alterable bonding energy of functional groups on the interface of nano-particle, variable transition energy of aromatic ring of electron mediator after linkage to nano-particle with surface-anchored enzyme, distinct mechanism of electron transferring and catalysis, crippled dynamics of redox procedure (i.e. electron shuttle between redox species and conductor) and improved acid–base endurance of magnetic nano-particle with tethered electron relay as well as protein. These unique features mostly resulted from adjacent ligation between redox site within electron mediator/enzyme and hetero-atoms of polymer as ligands. Investigation on these issues would be beneficial to have better understanding to the nature of metabolism of living organisms and would be helpful to secure an effective treatment for difficult and complicated disease.

Acknowledgements The study was financially supported by the National Natural Science Foundation of China (Nos. 31560249, 21363024).

References

1. S. Frasca, A.M. Milan, A. Guiet, C. Goebel, F. Pérez-Caballero, K. Stiba, S. Leimkühler, A. Fischer, U. Wollenberger, Electrochim. Acta **110**, 172 (2013)
2. A.A. Karyakin, Bioelectrochemistry **88**, 70 (2012)
3. M. Sosna, A. Bonamore, L. Gorton, A. Boffi, E.E. Ferapontova, Biosens. Bioelectron. **42**, 219 (2013)
4. E. Fernandez, J.T. Larsson, K.J. McLean, A.W. Munro, L. Gorton, C.V. Wachenfeldt, E.E. Ferapontova, Electrochim. Acta **110**, 86 (2013)
5. B. Royo, M. Sosna, A.C. Asencio, J.F. Moran, E.E. Ferapontova, J. Electroanal. Chem. **70**, 467 (2013)
6. J. Filip, J. Tkac, Bioelectrochemistry **96**, 14 (2014)
7. K. Chattopadhyay, S. Mazumdar, Bioelectrochemistry **53**, 17 (2000)
8. Y.T. Kong, M. Boopathi, Y.B. Shim, Biosens. Bioelectron. **19**, 227 (2003)
9. Y.D. Qian, X.Q. Xu, Q. Wang, P. Wu, H. Zhang, C.X. Cai, Phys. Chem. Chem. Phys. **15**, 16941 (2013)
10. D.S. Jiang, S.Y. Long, J. Huang, H.Y. Xiao, J.Y. Zhou, Biochem. Eng. J. **25**, 15 (2005)
11. L.R. Yang, C. Guo, S. Chen, F. Wang, J. Wang, Z.T. An, C.Z. Liu, H.Z. Liu, Ind. Eng. Chem. Res. **48**, 944 (2009)
12. D.P. Tang, R. Yuan, Y.Q. Chai, J. Phys. Chem. B **110**, 11640 (2006)
13. J.D. Qiu, H.P. Peng, R.P. Liang, Electrochem. Commun. **9**, 2734 (2007)
14. H. Wu, B.J. Sun, D.Q. Huang, Y.T. Liu, H. Zhang, Anal. Lett. **49**, 556 (2016)

15. H. Zeng, Y. Yang, S.X. Zhao, Y.H. Zhang, J. Inorg. Organomet. Polym. **27**, 1162 (2017)
16. Z.P. Kang, K.L. Jiao, R.Y. Peng, Z.Q. Hu, S.Q. Jiao, RSC Adv. **7**, 11872 (2017)
17. Z.P. Kang, K.L. Jiao, C. Yu, J. Dong, R.Y. Peng, Z.Q. Hu, S.Q. Jiao, RSC Adv. **7**, 4572 (2017)
18. Y. Yang, H. Zeng, W.S. Huo, Y.H. Zhang, J. Inorg. Organomet. Polym. **27**, 201 (2017)
19. Y. Yang, W.S. Huo, Z. Zhou, Q. Zhang, H. Zeng, Chin. J. Inorg. Chem. **32**, 2117 (2016) (**in Chinese**)
20. J.D. Qiu, H.P. Peng, R.P. Liang, X.H. Xia, Biosens. Bioelectron. **25**, 1447 (2010)
21. J. Huang, J.Y. Zhou, H.Y. Xiao, S.Y. Long, J.T. Wang, Acta. Chim. Sin. **63**, 1343 (2005) (**in Chinese**)
22. H.Y. Zhao, H.M. Zhou, J.X. Zhang, W. Zheng, Y.F. Zheng, Biosens. Bioelectron. **25**, 463 (2009)
23. K. Zhan, H.L. Liu, H. Zhang, Y.L. Chen, H.M. Ni, M. Wu, D.M. Sun, Y. Chen, J. Electroanal. Chem. **724**, 80 (2014)
24. B.L. Sun, X.D. Gou, R.B. Bai, A.A.A. Abdelmoaty, Y.L. Ma, X.P. Zheng, F.D. Hu, Mater. Sci. Eng. **74**, 515 (2016)
25. M. Klis, M. Karbarz, Z. Stojek, J. Rogalski, R. Bilewicz, J. Phys. Chem. B **113**, 6062 (2009)
26. Y.Z. Xian, Y. Xian, L.H. Zhou, F.H. Wu, Y. Ling, L.T. Jin, Electrochem. Commun. **9**, 142 (2007)
27. H. Huang, N.F. Hu, Y.H. Zeng, G. Zhou, Anal. Biochem. **308**, 141 (2002)
28. X.L. Ma, C.J. Ding, P. Zhang, W. Guo, H.X. Luo, Chin. J. Anal. Chem. **42**, 1332 (2014)
29. X.Q. Chen, H.Q. Yan, Z.F. Shi, Y.H. Feng, J.C. Li, Q. Lin, X.H. Wang, W. Sun, Polym. Bull. **74**, 75 (2017)
30. S.M. Dengale, A.K. Yagati, Y.H. Chung, J.H. Min, J.W. Choi, J. Nanosci. Nanotechnol. **13**, 6424 (2013)
31. X.M. Feng, Y.Y. Liu, Q.C. Kong, J.S. Ye, X.H. Chen, J.Q. Hu, Z.W. Chen, J. Solid State Electrochem. **14**, 923 (2010)